DALTON

2,2′:6′,2″:6″,2‴-Quaterpyridine (qtpy): a versatile ligand in metallosupramolecular chemistry; crystal and molecular structures of $[Ni(qtpy)(OH_2)_2][BF_4]_2$, $[Pd(qtpy)][PF_6]_2$, $[Cu_2(qtpy)_2][PF_6]_2$ and $[Ag_2(qtpy)_2][BF_4]_2$

Edwin C. Constable,*[a] Susan M. Elder,[b] Michael J. Hannon,[c] Avelino Martin,[b] Paul R. Raithby[b] and Derek A. Tocher[d]

[a] *Institut für Anorganische Chemie, Spitalstrasse 51, CH 4056 Basel, Switzerland*
[b] *Department of Chemistry, Lensfield Road, Cambridge CB2 1EW, UK*
[c] *Department of Chemistry, University of Warwick, Coventry CV4 7AL, UK*
[d] *Department of Chemistry, University College London, 20 Gordon Street, London WC1H 0AJ, UK*

The co-ordination behaviour of 2,2′:6′,2″:6″,2‴-quaterpyridine (qtpy) has been systematically studied. Double-helical dinuclear complexes were only obtained with ions bearing a low charge or a low charge-to-radius ratio and which have no electronically imposed preference for geometries in which the ligand can present a planar donor set. The double-helical complexes $[Cu_2(qtpy)_2][PF_6]_2$ and $[Ag_2(qtpy)_2][BF_4]_2$ have been structurally characterised, as have the mononuclear species $[Ni(qtpy)(OH_2)_2][BF_4]_2$ and $[Pd(qtpy)][PF_6]_2$. Complexes with zinc(II) and cadmium(II) are mononuclear but it is suggested that a double-helical dinuclear complex is formed with mercury(II).

Metallosupramolecular chemistry is concerned with the use of metal–ligand interactions to control the assembly of topologically or phenomenologically complex structures.[1–5] Strategically, the approach involves the design of building blocks which contain metal-binding domains together with such other functionality as is required in the desired metallosupramolecular product. Oligopyridines and related ligands have been incorporated as metal-binding domains into a wide range of such precursors which have been used to systematically assemble helicates,[2,6,7] knots,[8] receptors,[9] grids[10] and a cylinder[11] amongst other novel structures. The ligand 2,2′:6′,2″:6″,2‴-quaterpyridine (qtpy) and its substituted derivatives contain two directly linked didentate metal-binding domains and may be viewed as prototype helicands. In this paper we describe our detailed studies on the co-ordination behaviour of qtpy with a wide range of metal ions and probe the metal-centred features necessary for helication. Some of these results have been published previously in communication form.[12,13]

Experimental

Infrared spectra were recorded in compressed KBR discs on Perkin-Elmer 983 or Philips PU9624 Fourier-transform spectrophotometers, electronic spectra on a PU8730 spectrophotometer and ^1H NMR spectra on Bruker WM-250 or AM-400 spectrometers. Fast atom bombardment (FAB) spectra were recorded on a Kratos MS-50 spectrometer; the sample was loaded using acetonitrile as solvent, and 3-nitrobenzyl alcohol (noba) as supporting matrix. Electrochemical experiments were performed using an Autolab PGSTAT20 instrument or an AMEL system. A conventional three-electrode configuration was used with platinum-bead working and auxiliary electrodes and $Ag–Ag^+$ electrode as reference. The solvent was purified acetonitrile and the supporting electrolyte was 0.1 mol dm^{-3} $[NBu_4][BF_4]$ recrystallised twice from ethanol–water. Ferrocene was added at the end of each experiment as an internal standard. The compounds $[NiCl_2(PPh_3)_2]$,[14] and 6-chloro-2,2′-bipyridine[15] were prepared according to literature methods; PPh_3 and $NiCl_2·6H_2O$ were used as supplied (Aldrich). *N*,*N*-Dimethylformamide (dmf) was dried over molecular sieves (type 4A) prior to use. Zinc dust was washed with successive portions of dilute hydrochloric acid, distilled water, ethanol, acetone and diethyl ether immediately prior to use to remove the oxide layer.

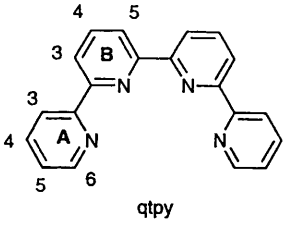

qtpy

Preparations

2,2′:6′,2″:6″,2‴-Quaterpyridine. A solution of $[NiCl_2(PPh_3)_2]$ (8.95 g, 13.7 mmol) and triphenylphosphine (7.67 g, 29.3 mmol) in dry, degassed dmf (75 cm^3) was heated to 50 °C with stirring under dinitrogen. The resulting blue solution was treated with zinc dust (1.29 g, 20.2 mmol); after 30 min a brick red colour had developed and a solution of 6-chloro-2,2′-bipyridine (2.61 g, 13.7 mmol) in dmf (15 cm^3) was added and the solution stirred at 50 °C for 24 h. After this period, the dark green solution was poured into aqueous ammonia (7% solution, 150 cm^3) and extracted with chloroform (3 × 100 cm^3). The aqueous solution was then treated with $NaBF_4$ (6 g, 54.5 mmol) and cooled, to give a precipitate containing green $[Ni(qtpy)(OH_2)_2][BF_4]_2$ and purple $[Ni(NH_3)_6][BF_4]_2$. The precipitates were isolated by filtration and then heated to reflux in acetonitrile–water (3:2, 25 cm^3) with potassium cyanide (5.2 g, 80 mmol) for 3 h. The solution turned yellow and the white solid which precipitated was collected by filtration, washed well with water and dried over P_2O_5 to give qtpy (0.81 g, 38%) (Found: C, 76.1; H, 4.4; N, 17.8. Calc. for $C_{20}H_{14}N_4·0.25H_2O$: C, 76.3; H, 4.6; N, 17.8%). IR (KBr): 1589w, 1578s, 1568s, 1561s, 1473w, 1447m, 1427s, 1382w, 1269m, 1112m, 1093w, 1074m, 1040w,

992w, 830w, 775vs, 739m, 635m and 617m cm^{-1}. Mass spectrum (EI): *m/z* 310 [*M*] and 232 [*M* − py] (py = pyridine). Mass spectrum (positive FAB): *m/z* 311 [M + H]. ^1H NMR ($CDCl_3$): δ 8.72 (1 H, d, *J* 4.6, H^{6A}), 8.68 (1 H, dd, *J* 7.8, 0.9, H^{5B}), 8.67 (1 H, dd, *J* 8.0, 0.9, H^{3A}), 8.48 (1 H, dd, *J* 7.8, 0.9, H^{3B}), 8.00 (1 H, t, *J* 7.8, H^{4B}), 7.89 (1 H, td, *J* 7.8, 1.8, H^{4A}) and 7.35 (1 H, ddd, *J* 7.5, 4.6, 1.2 Hz, H^{5B}). ^1H NMR (CD_3CN): δ 8.70 (3 H, m, $H^{3A,6A,5B}$), 8.51 (1 H, d, *J* 7.8, H^{3B}), 8.09 (1 H, t, *J* 7.9, H^{4B}), 7.97 (1 H, td, *J* 8.0 and 1.6 Hz, H^{4A}) and 7.44 (1 H, ddd, H^{5A}). ^1H NMR [$(CD_3)_2SO$]: δ 8.75 (1 H, d, *J* 4.8, H^{6A}), 8.70 (1 H, dd, *J* 7.9, 0.9, H^{3A}), 8.68 (1 H, d, *J* 7.5, H^{5B}), 8.50 (1 H, d, *J* 7.8, H^{3B}), 8.18 (1 H, t, *J* 7.8, H^{4B}), 8.04 (1 H, td, *J* 7.8, 1.8, H^{4A}) and 7.52 (1 H, ddd, *J* 7.5, 4.8, 1.1 Hz, H^{5A}).

Data for the intermediate green product [Ni(qtpy)$(OH_2)_2$][BF_4]$_2$: IR (KBr) 3172 (br), 1599s, 1579s, 1565w, 1490m, 1466s, 1441w, 1401s, 1084vs and 773s cm^{-1}; mass spectrum (positive FAB) *m/z* 368 {Ni(qtpy)}, 387 {Ni(qtpy)(OH_2)}, 403 {Ni(qtpy)$(OH_2)_2$} and 455 {Ni(qtpy)(BF_4)}.

[Pd(qtpy)][PF_6]$_2$. A mixture of qtpy (0.014 g, 0.045 mmol) and $Pd(O_2CMe)_2$ (0.010 g, 0.045 mmol) was heated to reflux in methanol (15 cm^3) for 3 h. The resulting yellow solution was filtered hot through Celite and then treated with an excess of methanolic [NH_4][PF_6]. An off white precipitate of [Pd(qtpy)][PF_6]$_2$ formed and was collected by filtration (0.014 g, 44%). IR (KBr): 1612m, 1599m, 1573m, 1488m, 1468s, 1415w, 1318m, 1252m, 1041m, 932m, 908m, 837vs, 785s, 669m and 559vs cm^{-1}. Mass spectrum (positive FAB): *m/z* 416 {Pd(qtpy)} and 561 {Pd(qtpy)(PF_6)}. ^1H NMR (CD_3CN): δ 8.66 (1 H, d, *J* 5.4, H^{6A}), 8.52 (1 H, t, *J* 8.3, H^{4B}), 8.45 (1 H, td, *J* 8.0, 1.5, H^{4A}), 8.38 (1 H, dd, *J* 8.0, 0.6, H^{3A}), 8.35 (1 H, dd, *J* 8.3, 0.9, $H^{5B,3B}$), 8.28 (1 H, dd, *J* 8.0, 0.8, $H^{3B,5B}$) and 7.93 (1 H, ddd, *J* 7.3, 5.5, 1.8 Hz, H^{5A}).

[Pt(qtpy)][PF_6]$_2$. A solution of qtpy (0.020 g, 0.065 mmol) and $K_2[PtCl_4]$ (0.035 g, 0.084 mmol) in aqueous acetonitrile (1 : 1, 10 cm^3) was heated to reflux for 12 h. The resulting yellow solution was filtered hot through cotton wool and the filtrate then treated with an excess of methanolic [NH_4][PF_6]. A yellow precipitate of [Pt(qtpy)][PF_6]$_2$ formed immediately and was collected by filtration, washed with diethyl ether and dried *in vacuo* (0.032 g, 68%) (Found: C, 29.7; H, 1.8; N 7.0. Calc. for $C_{20}H_{14}F_{12}N_4P_2Pt{\cdot}0.5H_2O$: C, 29.9; H, 1.9; N, 7.0%). IR (KBr): 1616m, 1603m, 1564w, 1469m, 1397w, 839vs, 785s and 559s cm^{-1}. Mass spectrum (positive FAB): *m/z* 505 {Pt(qtpy)} and 650 {Pt(qtpy)(PF_6)}. ^1H NMR (CD_3CN): δ 8.86 [1 H, d, *J* 5.6, ^3J(Pt–H) 27, H^{6A}], 8.50 (1 H, t, *J* 8.2, H^{4B}), 8.48 (1 H, td, *J* 7.8, 1.4, H^{4A}), 8.38 (1 H, dd, *J* 7.6, H^{3A}), 8.35 [1 H, dd, *J* 8.2, ^4J(Pt–H) 10, $H^{5B,3B}$], 8.24 [1 H, dd, *J* 8.2, ^4J(Pt– H^{3B}) 10, $H^{3B,5B}$] and 8.00 (1 H, ddd, *J* 7.7, 5.6, 1.5 Hz, H^{5A}).

[Zn(qtpy)$(O_2CMe)(OH_2)$][PF_6]. A solution of $Zn(O_2CMe)_2{\cdot}4H_2O$ (0.16 g, 0.65 mmol) and qtpy (0.020 g, 0.065 mmol) in methanol (10 cm^3) was heated under reflux for 2 h. The pale yellow solution was then treated with an excess of methanolic [NH_4][PF_6], and upon standing, yellow crystals separated which were collected by filtration and dried *in vacuo* to give [Zn(qtpy)$(O_2CMe)(OH_2)$][PF_6] (0.027 g, 70%) (Found: C, 44.3; H, 3.3; N, 9.2. Calc. for $C_{22}H_{19}F_6N_4O_3PZn$: C, 44.3; H, 3.2; N, 9.4%). IR (KBr): 3209 (br), 1625m, 1598m, 1581m, 1566m, 1490w, 1468s, 1440w, 1403w, 1384w, 1328w, 1033s, 1020w, 845vs, 776s, 667w, 656w and 559s cm^{-1}. Mass spectrum (positive FAB): *m/z* 374 {Zn(qtpy)}, 393 {Zn(qtpy)(OH_2)}, 433 {Zn(qtpy)(O_2CMe)} and 526 {Zn(qtpy)(noba)}.

[Zn(qtpy)$(OH_2)_2$][BF_4]$_2$. *Method 1.* A solution of [$Zn(OH_2)_6$][BF_4]$_2$ (0.022g, 0.064 mmol) and qtpy (0.020 g, 0.065 mmol) in ethanol (10 cm^3) was heated to reflux for 6 h. Upon cooling a white precipitate formed, which was collected by filtration and dried *in vacuo* to give [Zn(qtpy)$(OH_2)_2$][BF_4]$_2$ (0.032 g, 81%).

Method 2. A solution of [$Zn(OH_2)_6$][BF_4]$_2$ (0.041g, 0.118 mmol, excess) in acetonitrile (10 cm^3) was added to a solution of qtpy (0.020 g, 0.065 mmol) in methanol (10 cm^3) and the mixture heated under reflux for 1 h. The volume of the colourless solution was reduced and diethyl ether vapour diffused into the solution to give white crystals of [Zn(qtpy)$(OH_2)_2$][BF_4]$_2$ (0.026 g, 66%) (Found: C, 40.1; H, 3.2; N 9.8. Calc. for $C_{20}H_{18}B_2F_8N_4O_2Zn{\cdot}0.5H_2O$: C, 40.4; H, 3.1; N, 9.6%). IR (KBr): 3207 (br), 1600m, 1581m, 1567w, 1492w, 1469s, 1442w, 1124s, 1084vs, 1033s, 777s, 667w and 656w cm^{-1}. Mass spectrum (positive FAB): *m/z* 374 {Zn(qtpy)}, 393 {Zn(qtpy)(OH_2)}, 411 {Zn(qtpy)$(OH_2)_2$}, 461 {Zn(qtpy)(BF_4)} and 526 {Zn(qtpy)(noba)}. ^1H NMR (CD_3CN): δ 9.13 (1 H, d, *J* 5.6, H^{6A}), 8.50–8.65 (4 H, m, $H^{3A,3B,4B,5B}$), 8.39 (1 H, td, *J* 7.9, 1.5, H^{4A}) and 7.94 (1 H, ddd, *J* 7.7, 5.2, 1.0 Hz, H^{5A}).

[Cd(qtpy)$(O_2CMe)(OH_2)$][PF_6]. A solution of qtpy (0.015 g, 0.048 mmol) and $Cd(O_2CMe)_2{\cdot}2H_2O$ (0.013 g, 0.049 mmol) in methanol (10 cm^3) was heated under reflux for 12 h, after which period an excess of methanolic ammonium hexafluorophosphate was added to the colourless solution. A white precipitate slowly formed on cooling and was collected by filtration (0.015 g, 48%) (Found: C, 40.7; H, 2.9; N, 9.0. Calc. for $C_{22}H_{19}CdF_6N_4O_3$: C, 41.0; H, 3.0; N, 8.7%). IR (KBr): 3432 (br), 1596m, 1580s, 1570m, 1487w, 1464m, 1440m, 1417m, 845vs, 776s, 686w, 669w, 649w and 561m cm^{-1}. Mass spectrum (positive FAB): *m/z* 424 {Cd(qtpy)}, 439 {Cd(qtpy)(OH_2)}, 483 {Cd(qtpy)(O_2CMe)} and 576 {Cd(qtpy)(noba)}. ^1H NMR (CD_3CN): δ 8.57 (2 H, d, *J* 4.9, H^{6A}), 8.13 (6 H, m), 7.95 (4 H, m), 7.43 (2 H, ddd, *J* 6.7, 5.1, 1.9 Hz, H^{5A}) and 1.80 (3 H, s, O_2CMe).

[Hg(qtpy)][PF_6]$_2$. The compound $Hg(O_2CMe)_2$ (0.010 g, 0.032 mmol) and qtpy (0.010 g, 0.032 mmol) were heated to reflux in methanol (10 cm^3) for 10 h. The resulting colourless solution was treated with methanolic [NH_4][PF_6] and the white precipitate collected by filtration and recrystallised from acetonitrile by the slow diffusion of diethyl ether vapour to yield colourless blocks of [Hg(qtpy)][PF_6]$_2$ (0.016 g, 62%) (Found: C, 30.2; H, 1.6; N, 7.2. Calc. for $C_{20}H_{14}F_{12}HgN_4P_2$: C, 30.0; H, 1.8; N, 7.0%). IR (KBr): 1611w, 1579s, 1569s, 1471m, 1446s, 844vs, 785s and 550s cm^{-1}. Mass spectrum (positive FAB): 512 {Hg(qtpy)} and 657 {Hg(qtpy)(PF_6)}. ^1H NMR (CD_3CN): δ 8.81 (1 H, d, *J* 7.7, $H^{5B,3B}$), 8.46 (1 H, t, *J* 7.8, H^{4B}), 8.38 (1 H, d, *J* 7.8, $H^{3B,5B}$), 8.07 (1 H, d, *J* 7.9, H^{3A}), 7.79 (1 H, t, *J* 7.8 Hz, H^{4A}), 7.50 (1 H, d, H^{6A}) and 7.10 (1 H, dd, H^{5A}).

[Pb(qtpy)(O_2CMe)][PF_6]. A solution of qtpy (0.010 g, 0.032 mmol) and lead acetate (0.012 g, 0.032 mmol) in methanol (10 cm^3) was heated under reflux for 2 h. The colourless solution was filtered through Celite and the filtrate treated with an excess of methanolic ammonium hexafluorophosphate. Colourless needles precipitated on cooling (0.013 g, 56%) (Found: C, 36.4; H, 2.2; N, 7.6. Calc. for $C_{22}H_{17}F_6N_4O_2PPb$: C, 36.6; H, 2.4; N, 7.8%). IR (KBr): 1594m, 1570m, 1487w, 1463m, 1437m, 1400w, 1340w, 1290w, 1241w, 1197w, 1167w, 1105w, 1071w, 1043w, 1005w, 839vs, 775s and 558s cm^{-1}. Mass spectrum (positive FAB): *m/z* 518 {Pb(qtpy)} and 577 {Pb(qtpy)(O_2CMe)}. ^1H NMR (CD_3CN): δ 8.95 (2 H, d, *J* 5.6, H^{6A}), 8.54 (4 H, m, $H^{3B,5B}$), 8.42 (4 H, m, $H^{3A,4B}$), 8.18 (2 H, td, *J* 7.7, 1.4, H^{4A}), 7.73 (2 H, dd, *J* 7.4, 5.6 Hz, H^{5A}) and 1.46 (3 H, s, O_2CMe).

[H_2(qtpy)][PF_6]$_2$. *Method 1.* A solution of qtpy (0.01 g, 0.032 mmol) in dilute aqueous HCl (1 mol dm^{-3}, 10 cm^3) was treated with a methanolic solution of ammonium hexafluorophosphate to give an immediate white precipitate. The precipitate was collected by filtration, washed with diethyl ether and dried *in vacuo* to give [H_2(qtpy)][PF_6]$_2$ (0.015 g, 77%).

Method 2. A solution of $[Pt(cod)Cl_2]$ (cod = cycloocta-1,5-diene) (0.11g, 0.30 mmol) was heated to reflux in methanol (20 cm^3) until the solution was clear, after which qtpy (0.009 g, 0.03 mmol) was added and heating under reflux continued for 7 h. The solution was then cooled and treated with methanolic ammonium hexafluorophosphate. The precipitate which formed was collected and dried *in vacuo* to give $[H_2(qtpy)][PF_6]_2$ (0.003 g, 17%). IR (KBr): 1620m, 1608m, 1586s, 1566w, 1533m, 1523m, 1442s, 1387w, 1290w, 1268w, 843vs, 793s, 777m and 569s cm^{-1}. Mass spectrum (positive FAB): *m/z* 311 {H(qtpy)} and 456 $\{H_2(qtpy)(PF_6)\}$. ^1H NMR (CD_3CN): δ 9.10 (1 H, d, *J* 7.8, H^{5B}), 8.93 (1 H, d, *J* 5.7, H^{6A}), 8.75 (2 H, m, $H^{3A,4A}$), 8.47 (1 H, d, *J* 7.8, H^{3B}), 8.40 (1 H, t, *J* 7.8 Hz, H^{4B}) and 8.14 (1 H, ddd, H^{5A}).

$[Co(qtpy)(O_2CMe)(OH_2)][PF_6]$. The compound $Co(O_2CMe)_2{\cdot}4H_2O$ (0.016 g, 0.065 mmol) and qtpy (0.020 g, 0.065 mmol) were heated in methanol (10 cm^3) to reflux for 2 h, after which the resulting orange solution was treated with an excess of methanolic $[NH_4][PF_6]$ and allowed to cool. On standing, orange crystals of $[Co(qtpy)(O_2CMe)(OH_2)][PF_6]$ slowly formed (0.028 g, 73%) (Found: C, 44.1; H, 3.7; N, 8.9. Calc. for $C_{22}H_{19}CoF_6N_4O_3{\cdot}CH_3OH$: C, 44.3; H, 3.7; N, 9.0%). IR (KBr): 3230 (br), 1600s, 1578s, 1564s, 1491w, 1468s, 1441m, 1414m, 850vs, 775s, 571m and 556s cm^{-1}. Mass spectrum (positive FAB): *m/z* 369 {Co(qtpy)}, 384 {Co(qtpy)(OH)}, 428 {Co(qtpy)(O_2CMe)} and 521 {Co(qtpy)(noba)}.

$[Cu_2(qtpy)_2][PF_6]_2$. 2,2′:6′,2″:6″,2‴-Quaterpyridine (0.030 g, 0.097 mmol) and $[Cu(MeCN)_4][PF_6]$ (0.036 g, 0.097 mmol) were added to degassed methanol (10 cm^3) under dinitrogen. The resultant red solution was heated to reflux, with stirring, for 3 h after which it was cooled to −35 °C overnight. The deep red precipitate was collected by filtration, washed with diethyl ether and dried *in vacuo* (0.040 g, 80%) (Found: C, 46.1; H, 2.6; N, 10.8. Calc. for $C_{40}H_{28}Cu_2F_{12}N_8P_2$: C, 46.3; H, 2.7; N, 10.8%). IR (KBr): 1598s, 1572m, 1462s, 1440s, 1412w, 1389w, 1295w, 1248w, 1191w, 1160w, 841vs, 768s and 559s cm^{-1}. Mass spectrum (positive FAB): *m/z* 373 {Cu(qtpy)}, 437 $\{Cu_2(qtpy)\}$, 748 $\{Cu_2(qtpy)_2\}$ and 891 $\{Cu_2(qtpy)_2(PF_6)\}$. UV/VIS (MeCN): 543 (ε = 2800), 432 (4500), 303 (sh), 287 (35 000), 245 (31 000), 204 nm (50 000 cm^{-1} mol^{-1} dm^3).

$[Cu_2(qtpy)_2][BF_4]_2$. The complex was synthesised in an analogous way to $[Cu_2(qtpy)_2][PF_6]_2$ substituting $[Cu(MeCN)_4][BF_4]$ (0.031 g, 0.097 mmol) for the hexafluorophosphate salt. A deep brown precipitate of $[Cu_2(qtpy)_2][BF_4]_2$ (0.029 g, 65%) was obtained (Found: C, 51.6; H, 3.1; N, 12.9. Calc. for $C_{40}H_{28}B_2Cu_2F_8N_8{\cdot}CH_3CN{\cdot}OH_2$: C, 51.5; H, 3.4; N, 12.9%). IR (KBr): 1597s, 1570m, 1461s, 1438s, 1411w, 1385w, 1248w, 1084vs, 1054vs, 844w, 776s and 769s cm^{-1}. Mass spectrum (positive FAB): *m/z* 373 {Cu(qtpy)}, 435 $\{Cu_2(qtpy)\}$, 747 $\{Cu_2(qtpy)_2\}$ and 834 $\{Cu_2(qtpy)_2(BF_4)\}$. UV/VIS: identical to that of $[Cu_2(qtpy)_2][PF_6]_2$. ^1H NMR spectra: identical to those of $[Cu_2(qtpy)_2][PF_6]_2$.

$[Cu(qtpy)(MeOH)][PF_6]_2$. 2,2′:6′,2″:6″,2‴-Quaterpyridine (0.030 g, 0.097 mmol) and $Cu(O_2CMe)_2{\cdot}H_2O$ (0.019 g, 0.095 mmol) were heated to reflux in methanol (10 cm^3) for 3 h. Addition of a methanolic solution of an excess of $[NH_4][PF_6]$ to the blue solution, led to the formation of a blue precipitate of $[Cu(qtpy)(MeOH)][PF_6]_2$ (0.045 g, 67%) (Found: C, 36.3; H, 2.4; N, 8.2. Calc. for $C_{21}H_{24}CuF_{12}ON_4P_2$: C, 36.2; H, 2.6; N, 8.1%). IR (KBr): 1611m, 1604m, 1578m, 1495m, 1467s, 1326w, 1254m, 839vs, 785s and 558s cm^{-1}. Mass spectrum (positive FAB): *m/z* 373 {Cu(qtpy)} and 518 {Cu(qtpy)(PF_6)}. UV/VIS (MeCN): 630 (ε = 90), 352 (9000), 338 (9500), 293 (16 100), 260 (16 000), 243 nm (14 000 cm^{-1} mol^{-1} dm^3).

$[Ag_2(qtpy)_2][PF_6]_2$. 2,2′:6′,2″:6″,2‴-Quaterpyridine (0.030 g, 0.097 mmol) and $Ag(O_2CMe)$ (0.016 g, 0.097 mmol) were heated to reflux in methanol (10 cm^3) for 3 h. The straw coloured solution was filtered through cotton wool to remove some trace solid impurities and then treated with an excess of methanolic $[NH_4][PF_6]$ to yield immediately a white precipitate of $[Ag_2(qtpy)_2][PF_6]_2$ (0.031 g, 57%) (Found: C, 42.5; H, 2.5; N, 10.0. Calc. for $C_{40}H_{28}Ag_2F_{12}N_8P_2$: C, 42.6; H, 2.5; N, 10.0%). IR (KBr): 1592m, 1580m, 1568s, 1463s, 1438w, 1426s, 839vs, 770s and 559s cm^{-1}. Mass spectrum (positive FAB): *m/z* 417 {Ag(qtpy)}, 523 $\{Ag_2(qtpy)\}$, 728 $\{Ag(qtpy)_2\}$, 837 $\{Ag_2(qtpy)_2\}$ and 981 $\{Ag_2(qtpy)_2(PF_6)\}$.

$[Ag_2(qtpy)_2][BF_4]_2$. The tetrafluoroborate salt was synthesised in an analogous manner to $[Ag_2(qtpy)_2][PF_6]_2$. On the addition of an excess of methanolic $[NH_4][BF_4]$ to the straw coloured solution a pale yellow precipitate of $[Ag_2(qtpy)_2][BF_4]_2$ formed (0.036 g, 74%). IR (KBr): 1591w, 1578m, 1568s, 1473w, 1447w, 1427s, 1125s, 1084vs, 1039s and 771s cm^{-1}. Mass spectrum (positive FAB): *m/z* 417 {Ag(qtpy)}, 525 $\{Ag_2(qtpy)\}$, 727 $\{Ag(qtpy)_2\}$, 836 $\{Ag_2(qtpy)_2\}$ and 923 $\{Ag_2(qtpy)_2(BF_4)\}$. ^1H NMR spectra: identical to those of $[Ag_2(qtpy)_2][PF_6]_2$.

Crystal-structure Determinations of $[Ni(qtpy)(OH_2)_2][BF_4]_2$, $[Pd(qtpy)][PF_6]_2$, $[Cu_2(qtpy)_2][PF_6]_2$ and $[Ag_2(qtpy)_2][BF_4]_2$

Green crystals of $[Ni(qtpy)(OH_2)_2][BF_4]_2$ were obtained by slow cooling of a warm aqueous solution of the compound; off white, orange-red and pale yellow single crystals of $[Pd(qtpy)][PF_6]_2$, $[Cu_2(qtpy)_2][PF_6]_2$ and $[Ag_2(qtpy)_2][BF_4]_2$ respectively were obtained by the slow diffusion of diethyl ether vapour into acetonitrile solutions of the complexes.

Crystal data. $[Ni(qtpy)(OH_2)_2][BF_4]_2$. $C_{20}H_{18}B_2F_8N_4NiO_2$, green needles, crystal size 0.60 × 0.20 × 0.15 mm, M = 578.7, monoclinic, space group $P2_1/c$, a = 11.520(2), b = 12.744(2), c = 17.029(4) Å, β = 106.96(2)°, U = 2391 $Å^3$, $F(000)$ = 1168, Z = 4, D_c = 1.61 g cm^{-3}, μ(Mo-Kα) = 8.99 cm^{-1}.

$[Pd(qtpy)][PF_6]_2$. $C_{20}H_{14}F_{12}N_4P_2Pd$, off white needles, crystal size 0.40 × 0.15 × 0.15 mm, M = 706.7, monoclinic, space group $C2/c$, a = 17.485(2), b = 11.714(1), c = 14.261(2) Å, β = 127.60(1)°, U = 2314 $Å^3$, $F(000)$ = 1384, Z = 4, D_c = 2.03 g cm^{-3}, μ(Mo-Kα) = 10.4 cm^{-1}.

$[Cu_2(qtpy)_2][PF_6]_2$. $C_{40}H_{28}Cu_2F_{12}N_8P_2$, orange-red blocks, crystal size 0.13 × 0.13 × 0.40 mm, M = 1037.7, orthorhombic, space group $Pna2_1$, a = 23.974(5), b = 7.655(2), c = 22.002(4) Å, U = 4038 $Å^3$, $F(000)$ = 2080, Z = 4, D_c = 1.71 g cm^{-3}, μ(Mo-Kα) = 12.32 cm^{-1}.

$[Ag_2(qtpy)_2][BF_4]_2$. $C_{40}H_{28}Ag_2B_2F_8N_8$, pale yellow blocks, crystal size 0.25 × 0.20 × 0.15 mm, M = 1009.3, monoclinic, space group $C2/c$, a = 20.133(6), b = 18.489(6), c = 13.079(5) Å, β = 127.15(2)°, U = 3881 $Å^3$, $F(000)$ = 2000, Z = 4, D_c = 1.73 g cm^{-3}, μ(Mo-Kα) = 10.7 cm^{-1}.

Data collection and refinement. Crystals were mounted on glass fibres; geometric and intensity data were taken from these crystals using an automated four-circle Nicolet R3mV diffractometer {$[Ni(qtpy)(OH_2)_2][BF_4]_2$, $[Pd(qtpy)][PF_6]_2$ and $[Ag_2(qtpy)_2][BF_4]_2$} or a Stoe four-circle diffractometer {$[Cu_2(qtpy)_2][PF_6]_2$} equipped with graphite-monochromated Mo-Kα radiation. The ω–2θ technique was used to measure 4563 reflections (4139 unique) in the range $5 \leqslant 2\theta \leqslant 50°$ for $[Ni(qtpy)(OH_2)_2][BF_4]_2$, 4104 reflections (2645 unique) in the range $5 \leqslant 2\theta \leqslant 55°$ for $[Pd(qtpy)][PF_6]_2$, 3074 reflections (2715 unique) in the range $7 \leqslant 2\theta \leqslant 45°$ for $[Cu_2(qtpy)_2][PF_6]_2$ and 6923 reflections (3314 unique) in the range $11 \leqslant 2\theta \leqslant 22°$ for $[Ag_2(qtpy)_2][BF_4]_2$. The data were corrected for Lorentz and polarisation effects and an empirical absorption correction was applied in each case. The 2868 unique data with $I \geqslant 2\sigma(I)$ for $[Ni(qtpy)(OH_2)_2][BF_4]_2$, 2046

unique data with $I \geqslant 3\sigma(I)$ for $[Pd(qtpy)][PF_6]_2$, 2040 with $I \geqslant 4\sigma(I)$ for $[Cu_2(qtpy)_2][PF_6]_2$ and 1712 with $I \geqslant 2\sigma(I)$ for $[Ag_2(qtpy)_2][BF_4]_2$ were used to solve and refine the structures.

Structural analyses and refinement. The structures were solved by Patterson methods and developed using alternating cycles of least-squares refinement and Fourier-difference syntheses. The non-hydrogen atoms were refined anisotropically while hydrogen atoms were placed in idealised positions (C–H 0.96 Å) and assigned a common isotropic thermal parameter ($U = 0.08$ Å^2). The final R values were 0.0640 and 0.0660 and the final Fourier-difference maps were featureless with no peaks greater than 0.65 e Å^{-3} for $[Ni(qtpy)(OH_2)_2][BF_4]_2$; 0.0445 and 0.0511 and no peaks greater than 0.53 e Å^{-3} for $[Pd(qtpy)][PF_6]_2$; 0.0882 and 0.1063 with no peaks greater than 1.9 e Å^{-3} for $[Cu_2(qtpy)_2][PF_6]_2$; and 0.0728 and 0.0718 with no peaks greater than 0.86 e Å^{-3} for $[Ag_2(qtpy)_2][BF_4]_2$. Structure solution used SHELXTL-PLUS.[16] Selected bond lengths and angles for the complexes are presented in Table 1.

Atomic coordinates, thermal parameters and bond lengths and angles have been deposited at the Cambridge Crystallographic Data Centre (CCDC). See Instructions for Authors, *J. Chem. Soc., Dalton Trans.*, 1996, Issue 1. Any request to the CCDC for this material should quote the full literature citation and the reference number 186/69.

Discussion

The ligand qtpy has been found to form complexes with a variety of metal ions. In the majority of these complexes the qtpy adopts a near-planar conformation with all four nitrogen donors bonded to a single metal centre. This bonding mode is primarily associated with metal ions with a ligand-field preference for a square-planar or an octahedral co-ordination geometry and has been structurally confirmed for a range of metal ions.[13,17–26] More recently, we have described a unique complex in which a qtpy ligand co-ordinates to a six-co-ordinate metal centre in a hypodentate tridentate mode.[27,28] We have also recently reported that dinuclear double-helical complexes are obtained from the interaction of qtpy with copper(I) and silver(I) salts.[12] Results with substituted derivatives of qtpy have tended to parallel the co-ordination behaviour of the parent ligand.[20,29–34] The partitioning of qtpy into two didentate pseudo-bpy (bpy = 2,2′-bipyridine) metal-binding domains would lead to helication upon interaction with appropriate metal ions, and we have been attempting to define the precise requirements within the ligand and the metal centre which lead to such behaviour. In this paper we describe in full our systematic investigations of the co-ordination behaviour of qtpy with divalent d^8 metal ions and with divalent and monovalent d^{10} metal ions in an attempt to delineate precisely the requirements for helication.

The ligand qtpy was synthesised from 6-chloro-2,2′-bipyridine *via* an oxidative coupling reaction using a *stoichiometric* amount of a nickel(0) species generated from the reduction of $[NiCl_2(PPh_3)_2]$ in the presence of an excess of triphenylphosphine. The route described is a modification of our previously reported procedure[17] and improves the yield to 38%. As 6-chloro-2,2′-bipyridine is readily available,[15] this synthesis allows qtpy to be simply prepared in five steps from commercially available 2,2′-bipyridine with an overall yield of about 10%.

During the coupling reaction, the nickel(0) is oxidised to nickel(II), which can then co-ordinate to the qtpy ligand which has been formed. Work up of the reaction mixture yielded a dark coloured aqueous ammoniacal solution from which a mixture of emerald green and purple crystalline solids was obtained upon treatment with a methanolic solution of $NaBF_4$. If free qtpy is desired, demetallation of this mixture of products with potassium cyanide solution proceeds readily. The purple solid was shown to be $[Ni(NH_3)_6][BF_4]_2$. Mechanical separation of the crystalline products yielded the pure green compound, the positive FAB mass spectrum of which exhibits a main peak at m/z 368 corresponding to $[Ni(qtpy)]^+$ and weaker peaks at 387, 403 and 455 corresponding to $\{Ni(qtpy)(OH_2)\}$, $\{Ni(qtpy)(OH_2)_2\}$ and $\{Ni(qtpy)(BF_4)\}$ respectively, implying a formulation $[Ni(qtpy)(OH_2)_2][BF_4]_2$. The axial water ligands are weakly bound and readily dissociate in the mass spectrometer. This is a consistent feature of the positive FAB mass spectra of qtpy complexes and makes the presence and identification of the axial ligands difficult to prove. The IR spectrum of the complex shows qtpy stretches (1600–1500 cm^{-1}), a peak at 3172 cm^{-1} due to the co-ordinated water molecules and a strong peak at 1084 cm^{-1} due to the tetrafluoroborate counter ion.

We have previously structurally characterised the related cation $[Ni(qtpy)(MeCN)_2][PF_6]_2$ in which the metal ion is situated in a pseudo-octahedral co-ordination environment with the qtpy occupying four equatorial sites and the two solvent molecules occupying the axial sites.[17] In order to compare the structural effects of substituting the axial ligands in mononuclear qtpy complexes, we have now determined the crystal and molecular structure of the complex $[Ni(qtpy)(OH_2)_2][BF_4]_2$. As anticipated the cation $[Ni(qtpy)(OH_2)_2]^{2+}$ does indeed contain nickel(II) in a pseudo-octahedral co-ordination environment and the structure is shown in Fig. 1(*a*). A superimposition of the two structures (showing only the donor atoms of the axial ligands) is presented in Fig. 1(*b*). The

Table 1 Selected bond lengths (Å) and bond angles (°) in the co-ordination spheres of $[Ni(qtpy)(OH_2)_2][BF_4]_2$, $[Pd(qtpy)][PF_6]_2$, $[Cu_2(qtpy)_2][PF_6]_2$ and $[Ag_2(qtpy)_2][BF_4]_2$

$[Ni(qtpy)(OH_2)_2][BF_4]_2$			
Ni–O(1)	2.125(5)	Ni–O(2)	2.116(5)
Ni–N(1)	2.167(5)	Ni–N(2)	2.001(5)
Ni–N(3)	2.028(5)	Ni–N(4)	2.174(5)
O(1)–Ni–O(2)	167.0(2)	O(1)–Ni–N(1)	85.6(2)
O(2)–Ni–N(1)	88.6(2)	O(1)–Ni–N(2)	95.5(2)
O(2)–Ni–N(2)	94.5(2)	N(1)–Ni–N(2)	77.6(2)
O(1)–Ni–N(3)	93.9(2)	O(2)–Ni–N(3)	96.2(2)
N(1)–Ni–N(3)	155.5(2)	N(2)–Ni–N(3)	78.2(2)
O(1)–Ni–N(4)	85.7(2)	O(2)–Ni–N(4)	88.8(2)
N(1)–Ni–N(4)	127.8(2)	N(2)–Ni–N(4)	154.5(2)
N(3)–Ni–N(4)	76.4(2)		
$[Pd(qtpy)][PF_6]_2$			
Pd–N(1)	1.928(4)	Pd–N(2)	2.057(4)
Pd–N(1a)	1.928(4)	Pd–N(2a)	2.057(4)
N(1)–Pd–N(2)	80.5(2)	N(1)–Pd–N(1a)	81.2(2)
N(2)–Pd–N(1a)	161.7(2)	N(1)–Pd–N(2a)	161.7(2)
N(2)–Pd–N(2a)	117.7(2)	N(1a)–Pd–N(2a)	80.5(2)
$[Cu_2(qtpy)_2][PF_6]_2$			
Cu(1)–N(1)	2.077(16)	Cu(1)–N(2)	2.028(16)
Cu(1)–N(3)	2.039(15)	Cu(1)–N(4)	1.974(16)
Cu(2)–N(5)	2.057(17)	Cu(2)–N(6)	2.023(18)
Cu(2)–N(7)	2.071(13)	Cu(2)–N(8)	2.065(12)
N(1)–Cu(1)–N(2)	136.2(7)	N(1)–Cu(1)–N(3)	81.1(6)
N(2)–Cu(1)–N(3)	114.9(6)	N(1)–Cu(1)–N(4)	111.0(6)
N(2)–Cu(1)–N(4)	82.1(7)	N(3)–Cu(1)–N(4)	141.7(7)
N(5)–Cu(2)–N(6)	143.4(7)	N(5)–Cu(2)–N(7)	112.0(6)
N(6)–Cu(2)–N(7)	81.2(7)	N(5)–Cu(2)–N(8)	80.9(6)
N(6)–Cu(2)–N(8)	113.6(7)	N(7)–Cu(2)–N(8)	136.5(6)
$[Ag_2(qtpy)_2][BF_4]_2$			
Ag–N(1)	2.223(16)	Ag–N(2)	2.409(13)
Ag–N(3)	2.269(17)	Ag–N(4)	2.405(10)
Ag–Ag(a)	3.107(2)		
N(1)–Ag–N(2)	71.4(5)	N(1)–Ag–N(3)	150.1(3)
N(2)–Ag–N(3)	122.4(4)	N(1)–Ag–N(4)	118.0(4)
N(2)–Ag–N(4)	137.9(3)	N(3)–Ag–N(4)	71.5(4)

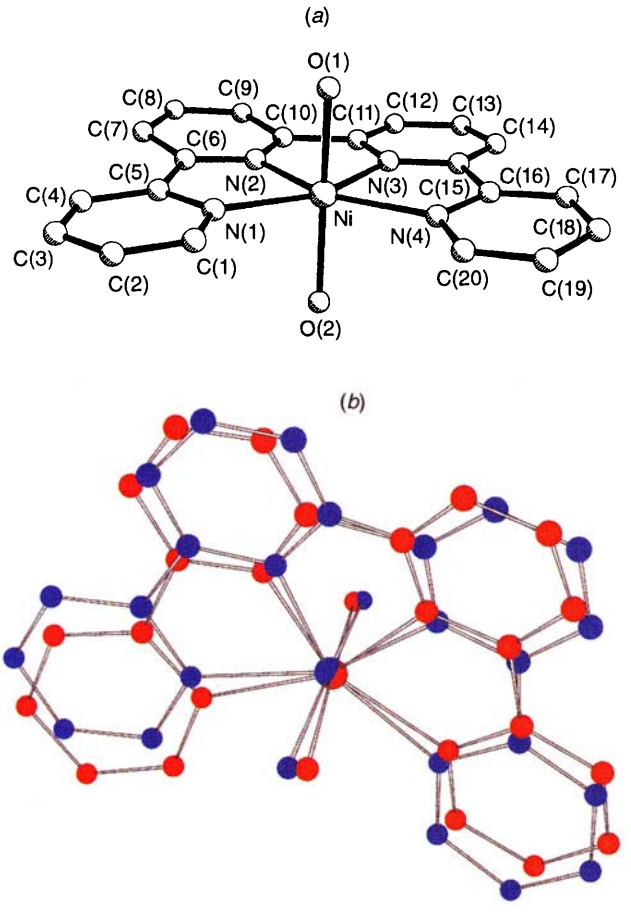

Fig. 1 (*a*) The crystal and molecular structure of the cation $[Ni(qtpy)(OH_2)_2]^{2+}$ present in the lattice of $[Ni(qtpy)(OH_2)_2][BF_4]_2$ showing the numbering scheme adopted. Hydrogen atoms have been omitted for clarity and (*b*) an overlay of the structures of the $[Ni(qtpy)(OH_2)_2]^{2+}$ (blue) and $[Ni(qtpy)(MeCN)_2]^{2+}$ (red) cations emphasising their similarity

two cations are remarkably similar. In both cases, the ligand is essentially planar and the geometry at the metal centre is close to octahedral. The bond lengths and angles (other than those to the axial ligands) are similar although the bond from the nickel ion to the terminal pyridine rings is slightly longer in the $[Ni(qtpy)(OH_2)_2]^{2+}$ cation. It is apparent that the small axial ligands have little effect on the metal–qtpy bonding despite the difference in donor atom (oxygen in water and nitrogen in acetonitrile). Nickel(II) is slightly too small to fit perfectly in the ligand cavity and, to bond effectively, the pyridine rings are required to flex inwards towards the metal ion. This results in small distortions to the ligand structure most easily quantified by a consideration of the bite angles (values in parentheses for the acetonitrile complex): N(1)–Ni–N(2) 77.6(2) (78.2), N(2)–Ni–N(3) 78.2(2) (77.6), N(3)–Ni–N(4) 76.4(2) (78.2°). Similar effects are observed in the structures of qtpy with other first-row transition-metal ions. The ligand distortions are insufficient to place all the pyridine rings equidistant from the metal centre and the metal–ligand bond lengths to the central pyridyl rings are constrained to be longer than those to the terminal rings. The two types of co-ordinate bond lengths [$Ni–N_{terminal}$ 2.167(5), 2.174(5) Å; $Ni–N_{central}$ 2.001(5), 2.028(5) Å] resemble those in $[Ni(qtpy)(MeCN)_2]^{2+}$ and fall either side of the value of 2.09 Å observed in the cation $[Ni(bpy)_3]^{2+}$.[35] Selected values of bond lengths and bond angles in the complex cation are presented in Table 1. To conclude, in nickel(II) complexes the qtpy behaves as a tetradentate ligand occupying the equatorial sites in near-octahedral cations.

In contrast to nickel(II), co-ordination of the other dipositive

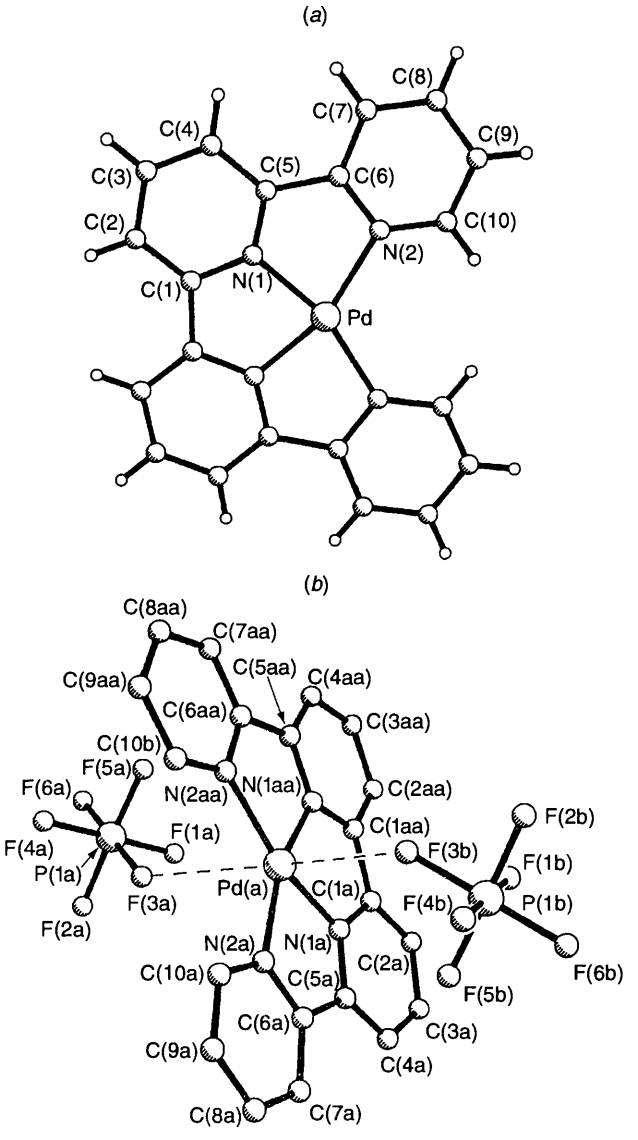

Fig. 2 (*a*) The crystal and molecular structure of the cation $[Pd(qtpy)]^{2+}$ present in the lattice of $[Pd(qtpy)][PF_6]_2$ showing the numbering scheme adopted and (*b*) the axial interactions with the counter ions

Group 10 metal ions to strong-field ligands such as qtpy is likely to lead to square-planar complexes and we have also investigated the interaction of these metal ions with qtpy. The reaction of palladium(II) acetate with qtpy in methanol solution gave a pale yellow solution from which an off-white solid precipitated upon the addition of a methanolic solution of $[NH_4][PF_6]$. Microanalytical data are consistent with a formulation $[Pd(qtpy)][PF_6]_2$ and this is supported by the observation of a peak corresponding to $\{Pd(qtpy)\}$ at m/z 416 in the FAB mass spectrum. Recrystallisation of the complex from acetonitrile by the slow diffusion of diethyl ether vapour yielded crystals suitable for X-ray diffraction analysis and we have determined the crystal and molecular structure of this complex. The co-ordination geometry of the cation $[Pd(qtpy)]^{2+}$ (Fig. 2) is indeed square planar and the ligand again binds in a planar tetradentate fashion. Interestingly, the palladium(II) ion in a square-planar geometry is effectively smaller than the nickel(II) ion in an octahedral environment {average M–N bond length in $[Pd(bpy)_2]^{2+}$ 2.03 Å, $[Ni(bpy)_3]^{2+}$ 2.09 Å}.[35] To bind to this smaller metal ion, the ligand is forced to flex even further inwards towards the metal ion. This results in both slightly shorter metal–ligand bond lengths [Pd–N(2) 2.057(4) and Pd–N(1), 1.928(4) Å] and larger bite angles [N(1)–Pd–N(2) 80.5(2), N(1)–Pd–N(1a) 81.2(2)°] than those observed in the

Table 2 Proton NMR spectroscopic data for various derivatives and complexes of qtpy in CD_3CN

	δ						
Compound	H^{6A}	H^{5A}	H^{4A}	H^{3A}	$H^{3B,5B}$	H^{4B}	$H^{5B,3B}$
qtpy	8.70	7.44	7.97	8.70	8.51	8.09	8.70
$[H_2(qtpy)][PF_6]_2$	8.93	8.14	8.75	8.75	8.47	8.40	9.10
$[H_2(qpy)][PF_6]_2$	8.92	8.10	8.72	8.72	8.45	8.37	9.01
$[Pd(qtpy)][PF_6]_2$	8.66	7.93	8.45	8.38	8.28	8.52	8.35
$[Pt(qtpy)][PF_6]_2$	8.86	8.00	8.48	8.38	8.24	8.50	8.35
$[Pb(qtpy)(O_2CMe)][PF_6]$	8.95	7.73	8.18	8.42	8.54	8.42	8.54
$[Hg(qtpy)][PF_6]_2$	7.50	7.10	7.79	8.07	8.38	8.46	8.81
$[Zn(qtpy)(OH_2)_2][BF_4]_2$	9.13	7.94	8.39		(8.50–8.65)		
$[Cd(qtpy)(O_2CMe)(OH_2)][PF_6]$	8.57	7.43	7.95		(8.13 and 7.95)		

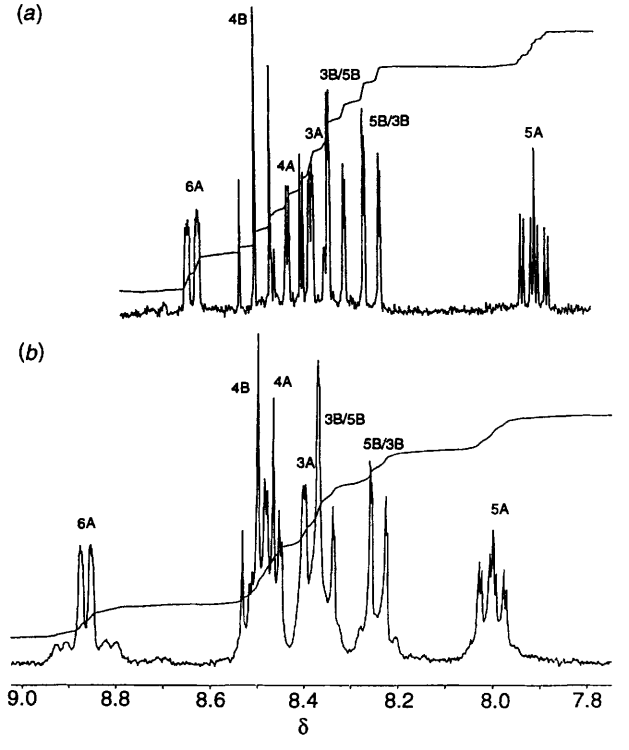

Fig. 3 The 250 MHz ^1H NMR spectrum of CD_3CN solutions of (*a*) $[Pd(qtpy)][PF_6]_2$ and (*b*) $[Pt(qtpy)][PF_6]_2$

nickel(II) species. Within the crystal lattice the palladium also exhibits two short interactions to the $[PF_6]^-$ anions [Pd · · · F 3.099(5) Å] [Fig. 2(*b*)].

The solution properties of this complex are also of interest and the ^1H NMR spectrum of the complex in acetonitrile solution is shown in Fig. 3(*a*). The spectrum is consistent with the maintenance of the square-planar geometry in solution. Seven distinct proton resonances are observed confirming that the ligand is symmetrical (on the NMR time-scale) in the solution species. The distinctive coupling patterns observed for pyridine rings make the assignment of the peaks straightforward and the chemical shift data, together with the assignments, are presented in Table 2. The pattern and precise chemical shifts of the complex are in marked contrast to those of the dinuclear double-helical copper(I) and silver(I) species[12] and suggests that the palladium complex remains square planar in solution.

We have also investigated the interaction of platinum(II) salts with quaterpyridine. Early reports established that platinum(II) formed complexes with qtpy,[36,37] and following our preliminary report of the palladium complex discussed above[13] a disordered structure of a $[Pt(qtpy)]^{2+}$ complex was described.[20] Within the constraints of the poorly refined platinum structure, the palladium and platinum cations are near identical in all important respects.

In attempts to avoid the formation of Magnus-type salts we have investigated the reaction of qtpy with a variety of platinum(II) starting materials. However, these studies were not entirely successful, and the reaction of $[Pt(MeCN)_2Cl_2]$ with qtpy in warm methanol gives rise to the green salt $[Pt(qtpy)][PtCl_4]$ whilst reaction with $[Pt(cod)Cl_2]$ under the same conditions yields only salts of the protonated ligand $[H_2(qtpy)]X_2$. Both of these species were identified by comparison with authentic samples. The salt $[Pd(qtpy)][PF_6]_2$ was obtained from $[Pt(qtpy)][PtCl_4]$ by a metathesis reaction. We wish to correct the previously reported ^1H NMR data for this species[20] which is incomplete and present the complete spectrum in Fig. 3(*b*); full chemical shift data and assignments for this complex in acetonitrile solution are presented in Table 2. A comparison with the data for the complex $[Pd(qtpy)][PF_6]_2$ shows that the shifts for the two complexes are very similar, strongly suggesting that the two complexes adopt similar structures in solution. Satellites are observed on the resonances corresponding to H^{6A}, H^{5A}, H^{3B} and H^{5B} due to coupling [^3J(Pt–H) 27 and ^4J(Pt–H) 10 Hz] to ^{195}Pt ($I = \frac{1}{2}$, 33.8% abundance). These coupling constants compare favourably with those observed in the platinum(II) complex of 6-(2-thienyl)-2,2′-bipyridine [^3J(Pt–H) 23 Hz].[38] In summary, all of the available evidence suggests that palladium(II) and platinum(II) complexes of qtpy are square planar and that no double-helical dinuclear species are formed.

This led us to consider separately the effects of charge and d-electron configuration upon helication. We had previously shown that qtpy behaved as a chelating tetradentate ligand with trivalent ions and that this was independent of the electronic configuration, occurring with both chromium(III) and yttrium(III).[23,24] While the Group 10 dications have a strong preference for octahedral (nickel) or square-planar (palladium and platinum) co-ordination a feature of the chemistry of the Group 12 dications is their tolerance of an array of geometries as there are no ligand-field imposed preferences with the d^{10} ions. This allows us to probe the effect of a change in electronic configuration with no change in charge. Accordingly, we have investigated the behaviour of Group 12 metal ions with qtpy.

Zinc(II) and cadmium(II) complexes formulated as $\{Zn(qtpy)Cl_2 \cdot 2H_2O\}$ and $\{Cd(qtpy)Cl_2 \cdot H_2O\}$, prepared from the reaction of qtpy with the relevant metal halide, have previously been reported[36] although no mercury(II) complexes of qtpy have been described. The reaction of zinc(II) acetate with qtpy in methanol gave a pale yellow solution from which a pale yellow crystalline material slowly precipitated after the addition of a methanolic solution of $[NH_4][PF_6]$. Partial microanalytical data for this salt are consistent with a formulation $\{Zn(qtpy)(O_2CMe)(OH_2)(PF_6)\}$ and the FAB mass spectrum shows peaks (with the correct isotopomer distribution) corresponding to $\{Zn(qtpy)\}$, $\{Zn(qtpy)(OH_2)\}$, $\{Zn(qtpy)(O_2CMe)\}$ and also a weaker peak corresponding to $\{Zn(qtpy)(noba)\}$ resulting from the association of the matrix with the complex in the spectrometer. No higher mass peaks are

observed. The IR spectrum of the complex shows qtpy and PF_6 absorptions and also a broad absorption centred at 3209 cm^{-1} assigned to co-ordinated water in addition to a band at 3450 cm^{-1} due to adventitious water adsorbed by the KBr. The region of the IR spectrum between 1500 and 1650 cm^{-1} is more complicated than in the nickel(II), platinum(II) and palladium(II) qtpy complexes discussed above and, in particular, there is a sharp absorption at 1625 cm^{-1} tentatively assigned to co-ordinated acetate. The precise identification of this mode is complicated by the superimposition of qtpy absorptions. The 250 MHz ^1H NMR spectrum of the complex in CD_3CN solution shows a peak at δ 1.67 assigned to the acetate group. The resonances due to qtpy are broadened, presumably as a result of a dynamic process in which axial ligands are being exchanged.

An acetate-free complex was prepared by the reaction of $[Zn(OH_2)_6][BF_4]_2$ with qtpy in ethanol or in a methanol–acetonitrile mixture. In ethanol a white product precipitated from the solution on cooling whilst with the latter solvent mixture, the same white compound was obtained by reducing the volume and slowly diffusing diethyl ether vapour into the concentrated solution. Partial microanalytical data for the product are consistent with a formulation $\{Zn(qtpy)(OH_2)_2(BF_4)_2\}$ and the FAB mass spectrum shows peaks (with the correct isotopomer distribution) corresponding to $\{Zn(qtpy)\}$, $\{Zn(qtpy)(OH_2)\}$, $\{Zn(qtpy)(OH_2)_2\}$, $\{Zn(qtpy)(BF_4)\}$ and, again, a weaker peak corresponding to {Zn(qtpy)(noba)}. The IR spectrum of the complex shows an absorption due to the tetrafluoroborate anion and a broad absorption centred at 3207 cm^{-1} due to co-ordinated water. The region of the infrared spectrum between 1500 and 1650 cm^{-1} is less complicated than in the $[Zn(qtpy)(O_2CMe)(OH_2)][PF_6]$ complex consistent with the absence of the acetate group. The 250 MHz ^1H NMR spectrum [Fig. 4(*a*)] of this tetrafluoroborate salt in CD_3CN solution is sharp and well resolved and indicates that the qtpy is symmetrical on the ^1H NMR spectroscopic time-scale. This is consistent with either a planar mononuclear or double-helical dinuclear complex. The resonances corresponding to H^{5A}, H^{4A} and H^{6A} are readily identified by their distinctive splitting patterns. The resonances corresponding to the other protons are observed as a multiplet at δ 8.5–8.65. On the basis of the mass spectrometric data we propose a mononuclear formulation and suggest that the two zinc(II) species contain the zinc ion in a pseudo-octahedral co-ordination geometry with a tetradentate qtpy ligand in the equatorial plane and the other two ligands above and below. In the case of $[Zn(qtpy)(OH_2)_2][BF_4]_2$ these ligands are two water molecules, while in the case of the salt $[Zn(qtpy)(O_2CMe)(OH_2)][PF_6]$ they are a water molecule and a monodentate acetate ligand.

Warming cadmium(II) acetate and qtpy in methanol solution gave a colourless solution from which a white hexafluorophosphate salt could be isolated. Partial microanalytical data on the white solid are consistent with a formulation $\{Cd(qtpy)(O_2CMe)(OH_2)(PF_6)\}$ and the FAB mass spectrum shows peaks with the correct isotopomer distribution corresponding to $\{Cd(qtpy)\}$, $\{Cd(qtpy)(OH_2)\}$ and $\{Cd(qtpy)(O_2CMe)\}$ and also a weaker peak corresponding to {Cd(qtpy)(noba)}. The IR spectrum of the complex shows peaks corresponding to (co-ordinated) qtpy and the hexafluorophosphate counter ion. Acetate stretches may also be present but since they fall in the same region as the qtpy stretches (1600–1500 cm^{-1}) they are difficult to assign with any degree of certainty. The 250 MHz ^1H NMR spectrum of the complex in CD_3CN solution is sharp and well resolved. The process which gives rise to the broadening in the spectrum of $[Zn(qtpy)(O_2CMe)(OH_2)][PF_6]$ either occurs rapidly on the ^1H NMR spectroscopic time-scale or the co-ordinated acetate is readily replaced by a water ligand. The aromatic region of the spectrum is presented in Fig. 4(*b*); in addition a singlet is observed at δ 1.80 assigned to acetate. Two of the naturally occurring isotopes of cadmium are spin active

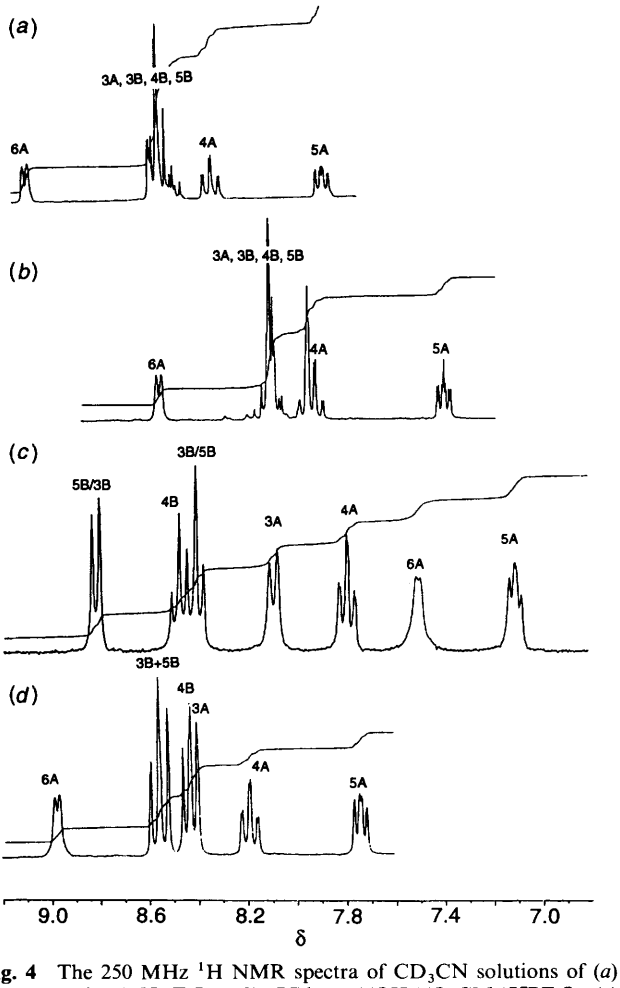

Fig. 4 The 250 MHz ^1H NMR spectra of CD_3CN solutions of (*a*) $[Zn(qtpy)(OH_2)_2][BF_4]_2$, (*b*) $[Cd(qtpy)(OH_2)(O_2CMe)][PF_6]$, (*c*) $\{[Hg(qtpy)][PF_6]_2\}_n$ and (*d*) $[Pb(qtpy)(O_2CMe)][PF_6]$

(^{111}Cd $I = \frac{1}{2}$, abundance 12.81%; ^{113}Cd $I = \frac{1}{2}$, abundance 12.22%) and very small satellite peaks may just be discerned. The resonances at δ 7.43 and δ 8.57 are readily assigned as H^{5A} and H^{6A} respectively from their distinctive splitting patterns. The resonances corresponding to H^{4A} (triplet of doublets) is evident on the upfield side of the multiplet at δ 7.95. The symmetry of the spectrum is again unsurprising. Other than a general upfield shift of about δ 0.5 the spectrum is very similar to that of the zinc complex $[Zn(qtpy)(OH_2)_2][BF_4]_2$. It seems likely that the structure of the cation is again pseudo-octahedral with a tetradentate qtpy ligand in the equatorial plane. As with the zinc complexes, there is no evidence for dinuclear helicate formation.

The reaction of mercury(II) acetate with qtpy in methanol gave a colourless solution from which a white solid precipitated instantly on the addition of an excess of methanolic $[NH_4][PF_6]$. The solid was recrystallised from acetonitrile solution by the slow diffusion of diethyl ether vapour to give colourless crystals. Partial microanalytical data on the crystalline product are consistent with a formulation $\{Hg(qtpy)(PF_6)_2\}$ and the FAB mass spectrum shows peaks (with the correct isotopic distribution) corresponding to $\{Hg(qtpy)\}$ and $\{Hg(qtpy)(PF_6)\}$. No higher mass peaks are observed. The IR spectrum shows stretches corresponding to co-ordinated qtpy and to the hexafluorophosphate counter ion. The absence of acetate is confirmed by the ^1H NMR spectrum of a CD_3CN solution of the complex which does not exhibit an acetate resonance. The aromatic region of the 250 MHz ^1H NMR spectrum in CD_3CN is shown in Fig. 4(*c*). Two of the isotopes of mercury are spin active (^{199}Hg $I = \frac{1}{2}$, abundance

17.0%; ^{201}Hg, $I = \frac{5}{2}$, abundance 13.2%), but satellites are not observed although some of the resonances (particularly H^{6A}) are slightly broadened. The spectrum, which exhibits a total of seven proton environments has been assigned with the aid of decoupling experiments. The full assignment is shown in Fig. 4(*c*) and the data are also presented in Table 2. In particular, the ^{1}H NMR spectrum is quite unlike the spectra of the zinc(II) and cadmium(II) complexes discussed above. In particular H^{6A}, which is usually observed at low field (even in the free ligand and the protonated complex), is shifted upfield. In related studies of double-helical dinuclear complexes involving 2,2′:6′,2″:6″,2‴:6‴,2⁗:6⁗,2⁗′-sexipyridine (spy) we have shown that the ^{1}H NMR spectra of the isostructural zinc(II), cadmium(II) and mercury(II) complexes are extremely similar.[39] Accordingly, we propose that the structure of the mercury(II) complex with qtpy differs from that of the zinc(II) and cadmium(II) species. The chemical shifts observed for this mercury(II) complex are completely different from those of the characterised square-planar palladium(II) and platinum(II) complexes, in particular, with respect to the upfield shifting of H^{6A}. This appears to preclude a square-planar formulation for the complex.

The analytical and mass spectrometric data suggest a formulation $[Hg(qtpy)][PF_6]_2$. The absence of 2:2 peaks in the mass spectrum would appear to exclude the possibility of a dinuclear double-helical co-ordination array although in a number of cases such peaks are found to be very low intensity. The principal difference in the co-ordination chemistry of mercury(II) from that of zinc(II) and cadmium(II) is the strong tendency to form complexes with four-co-ordinate tetrahedral mercury(II) centres. In the absence of confirmatory structural data we cannot make any definitive assignment of structure to this mercury(II) species, however, we tend towards a formulation as the dinuclear double-helical species $[Hg_2(qtpy)_2]^{4+}$ in which two tetrahedral mercury(II) centres are co-ordinated to a didentate bpy domain from each of the two ligand strands. In particular, the upfield shift of H^{6A} is reminiscent of that observed with the copper(I) and silver(I) species discussed below.

To investigate further the behaviour of qtpy with divalent metal ions with no ligand-field imposed geometrical preference we have also studied lead(II) complexes. The reaction of lead acetate with qtpy in methanol gave a colourless solution from which colourless, crystalline material slowly precipitated after the addition of methanolic $[NH_4][PF_6]$. Partial microanalysis of the material is consistent with a formulation $\{Pb(qtpy)(O_2CMe)(PF_6)\}$ and this is supported by the FAB mass spectrum which shows peaks corresponding to the species $\{Pb(qtpy)\}$ and $\{Pb(qtpy)(O_2CMe)\}$. The IR spectrum shows peaks corresponding to qtpy and to the hexafluorophosphate counter ion and is not inconsistent with the presence of acetate. The 250 MHz ^{1}H NMR spectrum of the complex in CD_3CN shows a resonance at δ1.46 corresponding to the acetate. The aromatic region of the 250 MHz ^{1}H NMR spectrum in CD_3CN is presented in Fig. 4(*d*) and has been assigned with the help of a 250 MHz COSY spectrum. The chemical shift data and the assignments are collected in Table 2. We suggest that the complex should be formulated as $[Pb(qtpy)(O_2CMe)][PF_6]$ and that the cation is square pyramidal with the qtpy ligand occupying the basal plane and the acetate in an axial position.

In order to ensure that the ^{1}H NMR and infrared spectra of the complexes reported herein are due to the metal complexes and not simply the protonated ligand and to confirm the assignment of the product from the reaction with $[Pt(cod)Cl_2]$, the hexafluorophosphate salt of the protonated ligand was prepared. We have previously prepared the chloride salt by the reaction of chromium(II) chloride with qtpy in methanol.[24] The hexafluorophosphate salt was precipitated from a solution of qtpy in dilute aqueous acid by the addition of an excess of methanolic $[NH_4][PF_6]$. The IR spectrum confirms that the ligand has been protonated; the stretching modes are shifted to slightly higher wavenumber with respect to free qtpy and there is a large peak due to the hexafluorophosphate counter ion. A stretch at 1620 cm^{-1} may represent an N–H bonding mode. The FAB mass spectrum shows a base peak corresponding to $\{H(qtpy)\}$ and a weaker peak corresponding to $\{H_2(qtpy)(PF_6)\}$. This is consistent with the structurally characterised species $[H_2(qpy)][PF_6]_2$ (qpy = 2,2′:6,2″:6″:2‴:6‴,2⁗-quinquepyridine) which shows only a peak corresponding to $\{H(qpy)\}$ in its FAB mass spectrum.[40] For comparison, data for the salt $[H_2(qtpy)][PF_6]_2$ are also presented in Table 2. Data for free qtpy in CD_3CN solution are also reported in Table 2. The spectrum is identical to that previously reported for solutions of the structurally characterised salt $[Y(qtpy)(NO_3)_2(H_2O)][NO_3]$,[23] suggesting that this complex dissociates in CD_3CN solution.

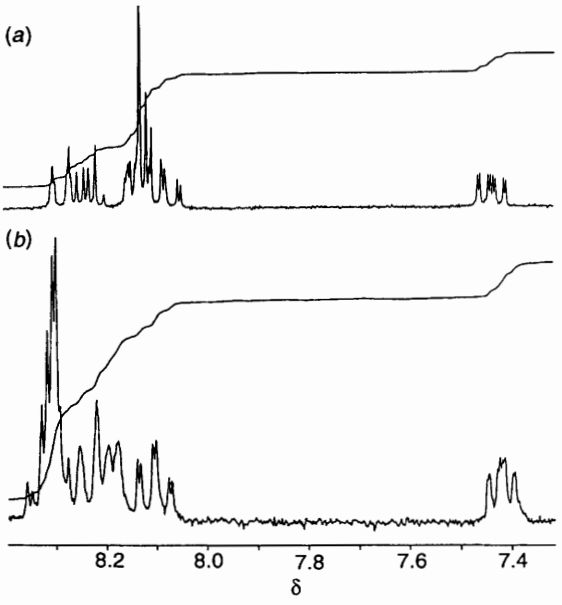

Fig. 5 The 250 MHz ^{1}H NMR spectra of $(CD_3)_2CO$ solutions of the double-helical complexes (*a*) $[Cu_2(qtpy)_2][PF_6]_2$ and (*b*) $[Ag_2(qtpy)_2][PF_6]_2$

Finally, we investigated the interaction of qtpy with univalent d^{10} metal ions. Previously, Lehn and co-workers[31,32] had shown that the preorganised ligand Me_4qtpy (5,5′,3″,5‴-tetramethyl-2,2′:6′,2″:6″,2‴-quaterpyridine) gave a dinuclear double-helical complex with copper(I). This behaviour was ascribed to the steric interactions between the methyl substituents of the two central rings preventing the adoption of a planar arrangement. Our more general strategy for the formation of helicates suggested that such species should be formed with qtpy *without* the use of preorganised ligands. The reaction of qtpy with solutions of $[Cu(MeCN)_4][PF_6]$ or $[Cu(MeCN)_4][BF_4]$ in MeOH resulted in the formation of red-brown solutions from which red-brown blocks of complexes of stoichiometry $\{Cu(qtpy)(PF_6)\}$ or $\{Cu(qtpy)(BF_4)\}$ were isolated. These complexes are indefinitely air-stable in the solid state and reasonably air-stable in solution. A similar reaction of qtpy with one equivalent of silver(I) acetate in methanol resulted in the formation of a pale coloured solution, from which salts of stoichiometry $\{Ag(qtpy)X\}$ (X = PF_6 or BF_4) could be obtained by the addition of $[NH_4][PF_6]$ or $[NH_4][BF_4]$ respectively. These complexes exhibited intense peaks in their FAB mass spectra corresponding to the species $\{M_2(qtpy)_2X_n\}$ (M = Cu or Ag; X = BF_4 or PF_6; n = 1 or 0). This is strong circumstantial evidence that the complexes are indeed double-helical dinuclear species. We note that extensive modelling studies have shown that with qtpy ligands a 2:2 stoichiometry is

only possible with double-helical arrangements of the ligands. The ^{1}H NMR spectra of solutions of these complexes in CD_3CN or $(CD_3)_2CO$ are similar and are presented in Figs. 5(*a*) and 5(*b*). The spectra clearly indicate that on the NMR time-scale the two bpy units of qtpy are equivalent.

The copper(I) complexes are deep red-brown, both in the solid state and in solution and the absorption spectrum (MeCN) shows a metal-to-ligand charge-transfer maximum at 432 nm (ε 4500 cm^{-1} mol^{-1} dm^3) and a further absorption at 543 nm (ε 2800 cm^{-1} mol^{-1} dm^3). This is strongly indicative of a tetrahedral arrangement of the four nitrogen donors about each copper(I) centre; for example, the mononuclear complex $[Cu(dmbpy)_2]^+$ (dmbpy = 6,6′-dimethyl-2,2′-bipyridine) exhibits a maximum at 454 nm (ε 6700 cm^{-1} mol^{-1} dm^3) whilst the double-helical species $[Cu_2(Me_4qtpy)_2]^{2+}$ and $[Cu_2(mbebm)_2]^{2+}$ {mbebm = 1,2-bis[6′-methyl(2,2′-bipyridyl)]-ethane} exhibit maxima at 454 (ε 12 700) and 445 nm (ε 9400 cm^{-1} mol^{-1} dm^3) respectively.

Recrystallisation of the salt $[Cu_2(qtpy)_2][PF_6]_2$ by the diffusion of diethyl ether vapour into an acetonitrile solution yielded red blocks of the complex, and we have determined the crystal and molecular structure. The structure of one of the two enantiomers of the binuclear $[Cu_2(qtpy)_2]^{2+}$ cation is shown in Fig. 6(*a*), together with a space-filling representation in Fig. 6(*b*). The cation is indeed double-helical with each copper co-ordinated to a didentate bpy unit from each ligand strand in a flattened tetrahedral geometry. The helication arises by twisting about the interannular C–C bonds. The bite angles to individual 2,2′-bipyridine residues range between 80.9(6) and 82.1(7)° and all of the copper–nitrogen bonded distances are within the expected range of 1.97(2)–2.08(2) Å. The differences between the two double-helical structures obtained with qtpy and Me_4qtpy are instructive. The copper–copper distance is significantly greater (3.90 Å) with the Me_4qtpy ligand than with the qtpy ligand (3.17 Å). This is the real effect of the sterically hindering methyl groups, they do not control the *formation* of the helix, but rather the metal–metal distance and the pitch of the helix. The removal of these steric interactions allows the flattening of the helix with a shorter metal–metal distance. The consequence of the flattening is a shallower pitch and smaller individual interannular C–C twistings between the two central rings of the ligands (75.6, 75.4° for Me_4qtpy; 40.2, 35.2° for qtpy). Interestingly, the interannular twistings between the terminal and adjacent rings are larger with qtpy than Me_4qtpy (9.1, 8.5, 9.6, 14.6 for Me_4qtpy; 17.5, 20.2, 18.8, 22.9° for qtpy). This is a result of the copper(I) attaining a distorted tetrahedral arrangement of the four donor atoms. The overall flattening of the helix also results in short graphitic contacts between approximately coplanar aromatic rings (3.68, 3.62, 3.89, 3.89 for Me_4qtpy; {1–5} 3.61, {2–6} 3.55, {3–8} 3.68, {4–7} 3.66 Å for qtpy; rings numbered according to the nitrogen atom that they contain). In each case, these are between the terminal pyridine of one ligand and one of the internal rings of the other ligand, and are significantly shorter for the qtpy complex. Following our initial report, the crystal structure of a $[Cu(ms_2qtpy)_2]^{2+}$ [ms_2qtpy = 4,4″-bis(methylsulfanyl)-2,2′:6′,2″:6″,2‴-quaterpyridine] salt has also been described.[33] The subtlety of the coding is illustrated in this latter structure; although there are no significant steric interactions between the methylsulfanyl substituents, the pitch of the double helix changes and the metal–metal distance is now 3.32 Å.

We have also determined the crystal and molecular structure of the salt $[Ag_2(qtpy)_2][BF_4]_2$ and the structure of one of the two enantiomers of the cation $[Ag_2(qtpy)_2]^{2+}$ is shown in Fig. 7(*a*). Once again, the cation is double-helical with each silver(I) centre co-ordinated to a didentate bpy domain from each of two qtpy ligands. Each silver atom is in an irregular four-co-ordinate environment and the Ag–N (2.223–2.409 Å) distances are unremarkable. Each bpy–silver interaction is associated with a bite angle of 70 ± 2° and the helical structure is achieved

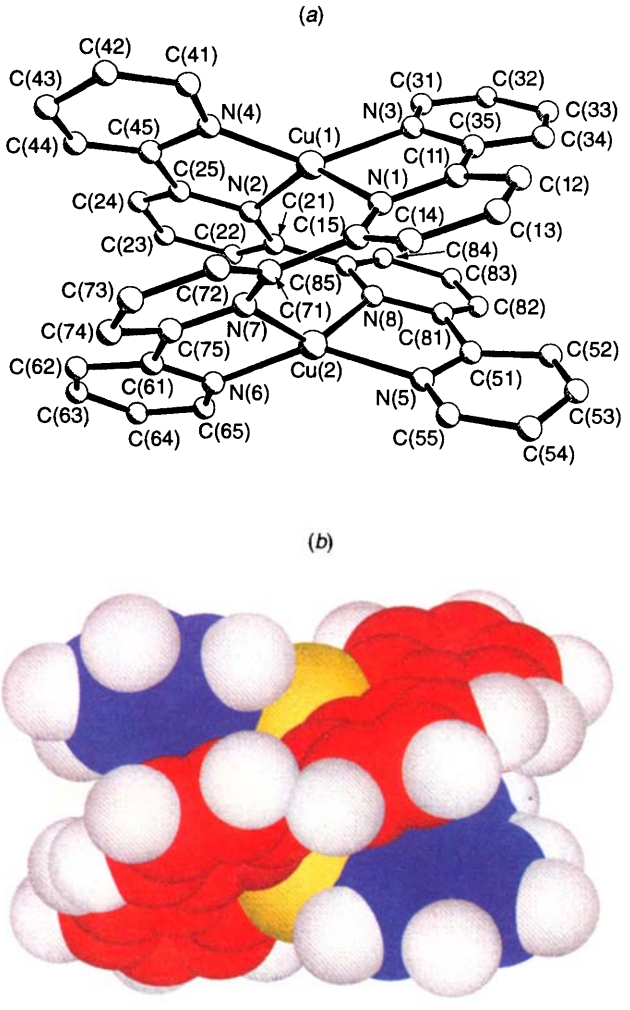

Fig. 6 (*a*) The crystal and molecular structure of one of the enantiomers of the cation $[Cu_2(qtpy)_2]^{2+}$ present in the lattice of $[Cu_2(qtpy)_2][PF_6]_2$ showing the numbering scheme adopted and (*b*) a space-filling representation showing the two qtpy strands and emphasising the helical structure. Hydrogen atoms have been omitted for clarity in both cases

by interannular twisting; each of the discrete bpy domains is slightly non-planar (13.0 and 13.5° interplanar angles) but the major twisting occurs between the two central pyridyl rings (45.1 and 46.9°). A space-filling representation of the double-helical cation is shown in Fig. 7(*b*). Pyridine rings of different ligands are approximately coplanar (8.1° between rings 1 and 3a, rings numbered according to the nitrogen atom that they contain), but the distance between the ring centroids is 4.53 Å, which argues against strong π-stacking interactions. The shortest contacts are of approximately 3.4 Å between overlapping edges. The two silver(I) centres are 3.107(2) Å apart in the cation. This short silver–silver contact is typical of that observed in many polynuclear disilver(I) complexes, and is not thought to be indicative of any particular intermetallic electronic interactions. Similar, and shorter, distances have been observed in other double-helical silver(I) complexes.[6]

It is worthy of note that although the silver(I) ion is larger than copper(I), the metal–metal distance is actually *shorter* than that observed in the complex $[Cu_2(qtpy)_2][PF_6]_2$ (Cu · · · Cu, 3.17 Å). We can now see that varying the metal ion size provides an alternative approach to peripheral substitution in controlling the pitch of the ligand. The introduction of the larger metal ion results in an increase in M–N distances and a lessening of the L–M–L bite angle, the consequence is that the metal–metal distance is simply controlled by the degree of twisting about the bond between the two bpy groups of each

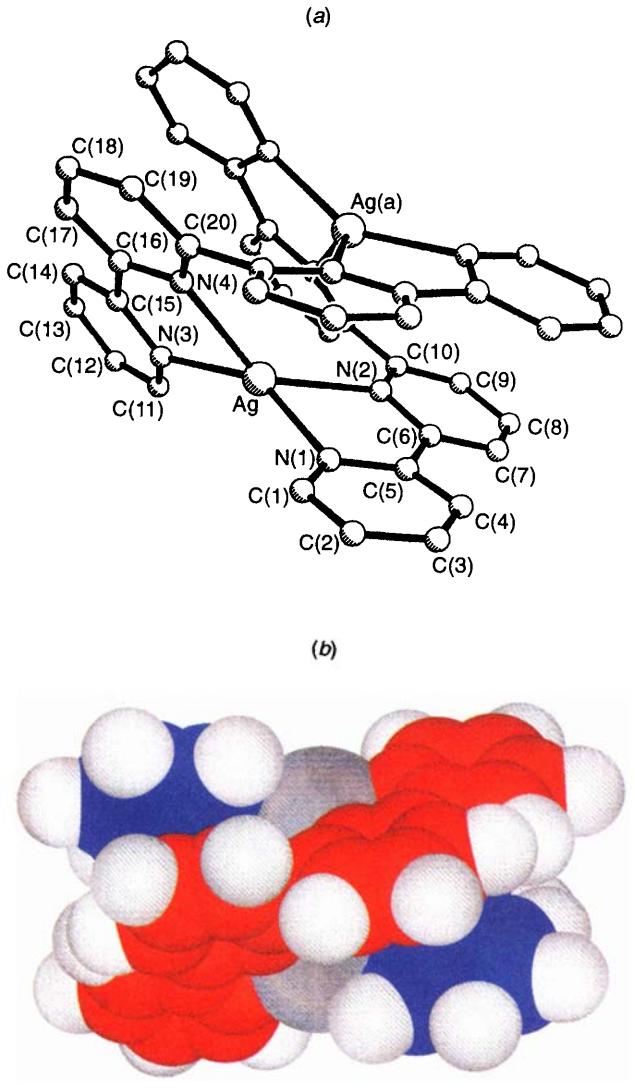

Fig. 7 (*a*) The crystal and molecular structure of one of the enantiomers of the cation $[Ag_2(qtpy)_2]^{2+}$ present in the lattice of $[Ag_2(qtpy)_2][BF_4]_2$ showing the numbering scheme adopted and (*b*) a space-filling representation showing the two qtpy strands and emphasising the helical structure. Hydrogen atoms have been omitted for clarity in both cases

ligand. However, the maximisation of the π overlap in the ligand occurs with a coplanar arrangement of rings, and intraligand electronic factors favour a minimisation of this twisting about the central interannular bond. The interannular twistings in the disilver complex (45.1, 46.9°) are indeed larger than in the dicopper(I) compound (35.2, 40.2°), but keeping these to a minimum results in very similar M–M distances.

The close contacts between the two metal centres in the qtpy complex has a number of consequences upon the *chemical* behaviour. Solutions of the complex cation $[Cu_2(Me_4qtpy)_2]^{2+}$ are electrochemically active, and exhibit two reversible redox processes generating dinuclear Cu^I–Cu^{II} and Cu^{II}–Cu^{II} species. The latter is unstable upon a chemical time-scale, and collapses to two mononuclear $[Cu(Me_4qtpy)]^{2+}$ cations. Reduction of the mononuclear species regenerates the dinuclear Cu^I–Cu^{II} and Cu^I–Cu^I species. In contrast, the cyclic voltammogram (MeCN, $[NBu_4][BF_4]$ supporting electrolyte, ferrocene–ferrocenium reference) of the complex $[Cu_2(qtpy)_2]^{2+}$ shows no evidence for the existence of a stable dinuclear mixed oxidation state complex and only two irreversible processes are observed at +0.05 and −0.42 V (Fig. 8). The instability of the mixed oxidation state in the case of the qtpy complex may be ascribed to the closer contact,

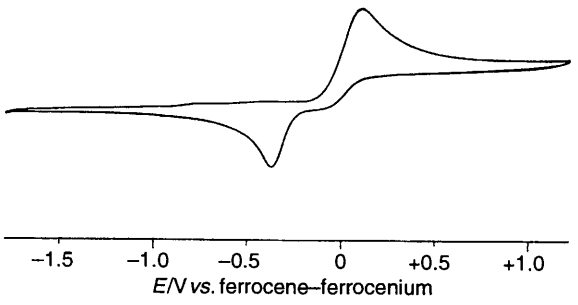

Fig. 8 Cyclic voltammogram of a solution of $[Cu_2(qtpy)_2][PF_6]_2$ in MeCN

and resulting electrostatic destabilisation, between the metal centres. Exactly the same electrochemical behaviour is observed upon starting with the structurally characterised[25] blue mononuclear copper(II) complex of 2,2′:6′,2″:6″,2‴-quaterpyridine. We have also studied the electrochemical behaviour of all of the other complexes discussed in this paper. In each case a number of reversible or quasi-reversible ligand-centred reductions are observed. There seem to be no systematic changes in these reductive processes between the mononuclear and dinuclear species and we have not studied these processes in detail. In the case of the silver complexes, irreversible absorption processes are also observed.

Conclusion

We have made a systematic study of the co-ordination behaviour of qtpy. With metal ions which possess an electronically imposed preference for an octahedral or square-planar co-ordination geometry, qtpy presents an essentially planar N_4 donor set. When there is no such electronically imposed preference, the consequences of co-ordination appear to be dependent upon the charge and the charge-to-radius ratio of the metal ion. Highly charged metal ions form mononuclear complexes with approximately planar N_4 donor sets from the ligand. Univalent d^{10} ions such as copper(I) and silver(I) give rise to double-helical dinuclear complexes. There is no need for preorganised ligands to be used for the formation of such structures. The role of the substituents in the preorganised ligands is not to control the assembly of the helix, but to control its pitch.

Acknowledgements

We should like to thank the Schweizerischer Nationalfonds zur Förderung der wissenschaftlichen Forschung (Grant number: 21-37325.93), the Science and Engineering Research Council (UK) and Ciba-Geigy plc for support, Johnson Matthey for the loan of precious metals, and Professors J.-P. Sauvage and V. Balzani for helpful discussions.

References

1 E. C. Constable, *Chem. Ind.*, 1994, 56.
2 E. C. Constable, *Prog. Inorg. Chem.*, 1994, **42**, 67.
3 M. Mascal, *Contemp. Org. Synth.*, 1994, 31.
4 V. Balzani, *Tetrahedron*, 1992, **48**, 10443.
5 G. Denti, S. Serroni, S. Campagna, A. Juris, M. Ciano and V. Balzani, in *Perspectives in Coordination Chemistry*, eds. A. F. Williams, C. Floriani and A. E. Merbach, VCHA, Basel, 1992, p. 153.
6 E. C. Constable, *Tetrahedron*, 1992, **48**, 10013; E. C. Constable and D. R. Smith, *The Polymeric Materials Encyclopedia*, CRC Press, Boca Raton, in the press; E. C. Constable, *Comprehensive Supramolecular Chemistry*, ed. J.-M. Lehn, Pergamon, in the press.
7 J.-M. Lehn, *Angew. Chem., Int. Ed. Engl.*, 1988, **27**, 89; J.-M. Lehn, in *Perspectives in Coordination Chemistry*, eds. A. F. Williams, C. Floriani and A. E. Merbach, VCHA, Basel, 1992, p. 447.

8 C. O. Dietrich-Buchecker and J.-P. Sauvage, *New J. Chem.*, 1992, **16**, 277; J.-P. Sauvage, J.-P. Collin, J.-C. Chambron, S. Guillerez, C. Coudret, V. Balzani, F. Barigelletti, L. De Cola and L. Flamigni, *Chem. Rev.*, 1994, **94**, 993.
9 M. S. Goodman, J. Weiss and A. D. Hamilton, *Tetrahedron Lett.*, 1994, **35**, 8943.
10 P. Baxter, J.-M. Lehn, J. Fischer and M.-T. Youinou, *Angew. Chem., Int. Ed. Engl.*, 1994, **33**, 2284.
11 P. Baxter, J.-M. Lehn, A. DeCian and J. Fischer, *Angew. Chem., Int. Ed. Engl.*, 1993, **32**, 69.
12 E. C. Constable, M. J. Hannon, A. Martin, P. R. Raithby and D. A. Tocher, *Polyhedron*, 1992, **11**, 2967.
13 E. C. Constable, S. M. Elder, J. Healy, M. D. Ward and D. A. Tocher, *J. Am. Chem. Soc.*, 1990, **112**, 4590.
14 F. A. Cotton, O. D. Faut and D. M. L. Goodgame, *J. Am. Chem. Soc.*, 1961, **83**, 344.
15 A. J. Downard, G. E. Honey, L. F. Phillips and P. J. Steel, *Inorg. Chem.*, 1991, **30**, 2259.
16 G. M. Sheldrick, SHELXTL-PLUS, University of Göttingen, 1986.
17 E. C. Constable, S. M. Elder, J. Healy and D. A. Tocher, *J. Chem. Soc., Dalton Trans.*, 1988, 1669.
18 C.-M. Che, Y.-P. Wang, K.-S. Yeung, K.-Y. Wong and S.-M. Peng, *J. Chem. Soc., Dalton Trans.*, 1992, 2675.
19 C.-W. Chan, C.-M. Che and S.-M. Peng, *Polyhedron*, 1993, **12**, 2169.
20 C.-W. Chan, C.-M. Che, M.-C. Cheng and Y.-P. Wang, *Inorg. Chem.*, 1992, **31**, 4874.
21 E. N. Maslen, C. L. Raston and A. H. White, *J. Chem. Soc., Dalton Trans.*, 1975, 323.
22 S. M. Yang, K. K. Cheung and C.-M. Che, *J. Chem. Soc., Dalton Trans.*, 1993, 3315.
23 E. C. Constable, S. M. Elder and D. A. Tocher, *Polyhedron*, 1992, **11**, 2599.
24 E. C. Constable, S. M. Elder and D. A. Tocher, *Polyhedron*, 1992, **11**, 1337.
25 W. von Henke, S. Kremer and D. Reinen, *Z. Anorg. Allg. Chem.*, 1982, **491**, 124.
26 C. M. Che, C. W. Chan, S. M. Yang, C. X. Guo, C. Y. Lee and S. M. Peng, *J. Chem. Soc., Dalton Trans.*, 1995, 2961.
27 E. C. Constable, M. J. Hannon, A. M. W. Cargill Thompson, D. A. Tocher and J. V. Walker, *Supramol. Chem.*, 1993, **2**, 243.
28 R. Chotalia, E. C. Constable, M. J. Hannon and D. A. Tocher, *J. Chem. Soc., Dalton Trans.*, 1995, 3571.
29 E. C. Constable, P. Harverson, D. R. Smith and L. A. Whall, *Tetrahedron*, 1994, **50**, 7799.
30 E. C. Constable, M. J. Hannon and D. R. Smith, *Tetrahedron Lett.*, 1994, **35**, 6657.
31 J.-P. Gisselbrecht, M. Gross, J.-M. Lehn, J.-P. Sauvage, R. Ziessel, C. Piccinni-Leopardi, J. M. Arrieta, G. Germain and M. Van Meerssche, *Nouv. J. Chim.*, 1984, **8**, 661.
32 J.-M. Lehn, J.-P. Sauvage, J. Simon, R. Ziessel, C. Piccinni-Leopardi, G. Germain, J.-P. Declercq and M. Van Meerssche, *Nouv. J. Chim.*, 1983, **7**, 413.
33 K. T. Potts, M. Keshavarzk, F. S. Tham, H. D. Abruna and C. R. Arana, *Inorg. Chem.*, 1993, **32**, 4422.
34 C.-W. Chan, T.-F. Lai and C.-M. Che, *J. Chem. Soc., Dalton Trans.*, 1994, 895.
35 E. C. Constable, *Adv. Inorg. Chem.*, 1989, **34**, 1.
36 G. T. Morgan and F. H. Burstall, *J. Chem. Soc.*, 1938, 1672, 1675.
37 H. C. Lip and R. A. Plowman, *Aust. J. Chem.*, 1975, **28**, 893.
38 E. C. Constable, R. P. G. Henney, P. R. Raithby and L. R. Sousa, *J. Chem. Soc., Dalton Trans.*, 1992, 2251.
39 R. Chotalia, E. C. Constable, M. Neuburger, D. R. Smith and M. Zehnder, unpublished work.
40 E. C. Constable, S. M. Elder, J. V. Walker, P. D. Wood and D. A. Tocher, *J. Chem. Soc., Chem. Commun.*, 1992, 229.

Received 8*th January* 1996; *Paper* 6/00165C